

**MODELING FRAMEWORKS FOR REPRESENTING THE MECHANICAL  
BEHAVIOR OF TISSUES WITH A SPECIFIC LOOK AT VASCULATURE**

A Thesis

by

ALEXANDER PAUL ANDERSOHN

Submitted to the Office of Graduate and Professional Studies of  
Texas A&M University  
in partial fulfillment of the requirements for the degree of

MASTER OF SCIENCE

Chair of Committee,	John C. Criscione
Committee Members,	Arun Srinivasa
	Michael R. Moreno
Head of Department,	Gerard L. Coté

December 2013

Major Subject: Biomedical Engineering

Copyright 2013 Alexander Paul Andersohn

## **ABSTRACT**

Many mechanistic models aimed at predicting tissue behavior attempt to connect constitutive factors (such as effects due to collagen or fibrin concentrations) with the overall tissue behavior. Such a link between constitutive and material behaviors would allow for a better understanding of the mechanobiology of diseased states and how one might return the tissue to a healthy state. Therefore, a literature search into present mechanistic models was performed and yielded a variety of models that were analyzed in order to determine their uniqueness, a requisite characteristic for this aim. It was found that many of these models did not make uniqueness a defining characteristic in their development and thus cannot be used for multiscale modeling (connecting constitutive behavior to material behavior). The literature search was then extended and narrowed to specifically analyze mechanical models describing vascular wall behavior. Once again, it was found that uniqueness was lacking in these models. To develop a unique model for inflation strains, an inflation experiment utilizing a bladder, syringe, and a pressure sensor was conducted to provide pressure vs. volume data for a sheep aorta. The data was then used to develop a unique model for inflation strains in an aorta utilizing a constitutive framework developed by Dr. John Criscione.

## **DEDICATION**

To my parents, I would not be where I am today without your guidance. Thank  
you so much.

## **ACKNOWLEDGEMENTS**

I would like to thank my committee chair, Dr. Criscione for all of the support and guidance he has provided in the course of this thesis and my education. I would also like to thank my other committee members, Dr. Srinivasa and Dr. Moreno, for their aid and encouragement throughout the development of this thesis. I likewise appreciate Dr. Partha Mukherjee for his willingness to replace Dr. Srinivasa at my defense.

Thanks also go to my friends and family for all they have done to support and encourage me. I would like to also extend my thanks to the faculty and staff in the Biomedical Engineering department for making my time at Texas A&M University a great experience.

Finally, thank you to my mother and father for their incredible financial and emotional backing of my goals. I appreciate everything you have done on my behalf.

## TABLE OF CONTENTS

	Page
ABSTRACT .....	ii
DEDICATION .....	iii
ACKNOWLEDGEMENTS .....	iv
TABLE OF CONTENTS .....	v
LIST OF FIGURES .....	vii
LIST OF TABLES .....	viii
1. INTRODUCTION .....	1
2. INVESTIGATION INTO DETERMINABILITY .....	2
2.1 Introduction .....	2
2.2 Separation of the Scales of Interest .....	3
2.3 Variation and Uniformity .....	6
2.4 Uniqueness and Completeness .....	7
3. CRITICAL EVALUATION OF MECHANISTIC MODELS .....	9
3.1 Literature Search and Analysis .....	9
3.2 Results and Discussion .....	10
4. CRITICAL REVIEW SPECIFIED TO ARTERIAL MODELS .....	15
4.1 Introduction .....	15
4.2 Delfino et al. (1997) .....	16
4.3 Holzapfel, Gasser, Stadler (2002) .....	17
4.4 Horgan, Saccomandi (2003) .....	18
4.5 Pena et al. (2010) .....	20
4.6 Zulliger et al. (2004) .....	21
4.7 Conclusion .....	22

5. MESOSCALE AND THE REPRESENTATIVE VOLUME ELEMENT .....	24
5.1 Defining the Representative Volume Element .....	24
5.2 Comparing the RVE and the Mesoscale .....	26
6. ENERGY FUNCTION FIT TO SHEEP AORTA INFLATION DATA .....	29
6.1 Method of Data Collection .....	29
6.2 Constitutive Framework .....	30
6.3 Results .....	34
6.4 Concluding Remarks .....	41
7. CONCLUSION .....	43
REFERENCES .....	44

## LIST OF FIGURES

	Page
Figure 1: Graphical Representation of Length Scales of Interest .....	5
Figure 2: Degeneracy Plot across Length Scales.....	7
Figure 3: Pressure vs. Beta for Sheep Aortas Tested in Inflation.....	36
Figure 4: $\delta w/\delta\text{Beta}$ vs Beta.....	38
Figure 5: Pressure vs Beta Fit for 80mmHg – 120mmHg Range.....	39
Figure 6: $\delta W/\delta\text{Gamma3}$ vs Gamma3.....	41

## LIST OF TABLES

	Page
Table 1: Separation of Length Scales of Interest .....	4
Table 2: List of Mechanistic Models with Characterizations .....	10
Table 3: List of Arterial Mechanics Models with Characterizations .....	16
Table 4: $P_i$ and $B_i$ for Tested Sheep Aortas .....	37



## 1. INTRODUCTION

One of the main objectives of biomechanics is to develop mathematical models that fully represent and can predict tissue behavior when it is exposed to certain stresses or strains. Having read many articles presenting various versions of these models, it has become evident that not only is this representation sought, but also how microscale constituents such as collagen and fibrin fibers affect this overall behavior. Many models attempt to determine this relationship and account for the effects of such constituents in their strain energy functions. This link between constituent behavior and material behavior would allow for a better understanding of the mechanobiology of diseased states and means to return the body to its healthy state. The process by which the overall material behavior can be expressed in terms that are influenced by the microscale components of the tissue is termed multiscale modeling. Unfortunately, many of the models cannot fully characterize the behavior whether it is due to a subset of materials that cannot be represented or due to increasing effects of measurement error leading to indeterminability. With this in mind, I determined that a discussion on the features of mechanistic models that would allow for such an aim to be achieved was desperately needed. This thesis lays the groundwork for such a discussion by providing clear definitions for the scales of interest, analyses of several models on their applicability to multiscale modeling, and the presentation of a model developed from a constitutive approach that can allow for uniqueness and multiscale modeling.

## 2. INVESTIGATION INTO DETERMINABILITY

### *2.1 Introduction*

When modeling any material, it should be evident that data fitting is a necessity. The more pertinent question for a specific application is: “is data fitting necessary AND sufficient?” If the answer is yes, then any model that fits the data will be a great choice. For a simplified example of an application where data fitting is necessary and sufficient, consider the making of sundials. It is irrelevant whether the earth spins as it orbits the sun or if the sun is pulled by a chariot across the sky. With any model that fits observational data from a particular earthly location, a sun dial can be constructed. Likewise, if the designer of an arterial stent is only interested in the luminal forces needed to distend an artery, then any arterial model that fits distention data is acceptable. If data fitting was necessary and sufficient for all applications, then modeling would not require expertise—all a reviewer would need to do is consider how the model fits the data, and provided that results are presented appropriately, it does not take much skill to compare model results to experimental results. Alas, true applications of modeling (i.e., applications where modeling is necessary) are not so simple; data fitting alone is insufficient. This is the case for multiscale modeling when a link between material behavior and material composition is sought. For such an endeavor, a model of material behavior must be unique and determinable. Simply fitting the data with a non-unique model is insufficient because a physical link is sought between constituent behavior and constitutive behavior and one cannot link definite constituents to indefinite constitutive

relations. The characteristics necessary for multiscale modeling are a focus of this paper; yet the results are applicable whenever material behavior is to be “determined” as opposed to “fit”. The later can be done with an “indeterminable” representation whereas the former cannot.

## *2.2 Separation of the Scales of Interest*

There are many length and time scales of interest when considering modeling of biomedical phenomena. Therefore, when attempting to utilize a mechanical model to represent physical phenomena, it is useful to define which scales characterize the behavior being modeled (see Table 1). The nano-scale is defined as having primary characteristics at lengths of  $10^{-9}$  m. Similarly, the micro-scale is defined as having primary characteristics of  $10^{-6}$  m. These two scales, together, will make up what I will define as the level for defining the behavior of constituents. After looking into alternative definitions of the mesoscale, I offer one more suited for the purposes of multiscale modeling. I propose that the mesoscale be defined such that the region of interest is large enough to contain all constituents in suitable number to be averaged (often referred to as the representative volume element, RVE) but small enough to be independent of body geometry. The systemic scale is defined as having characteristics on the scale of organ systems and represents lengths that are multiples of the mesoscale. The macro-scale represents the length scale of the organism or body of interest. These larger length scales, systemic and macro, represent the behavior of the “body” as a whole (by body I may mean a material body or perhaps an entire organism). Beyond the

macro-scale, physical models tend to be n-Body problems (e.g. populations). Therefore, I will consider an appropriate triad of scales that represent behaviors of interest to multiscale modeling – the constituent scale (nano and micro scales), the material scale (mesoscale), and the body scale (systemic and macro scales).

Scales	Triad of Interest
Nano-scale	Constituent scale
Micro-scale	
Mesoscale	Material scale / Tissue scale
Systemic scale	Body scale
Macro-scale	

**Table 1: Separation of Length Scales of Interest.** Summary of the scales of interest to multiscale modeling

At the core of this triad is the mesoscale, which is representative of the material behavior yet independent of body geometry.

For illustration of these scales, consider a vessel with fluid flow through it (e.g. a blood vessel) that branches at a bifurcation into two, smaller vessels, as shown in Figure 1. We can see that, when considering the whole bifurcation, the flow varies significantly – we can identify distinct directions of flow at different locations. Specifically, the flow varies with position or with geometry of the vessel. However, if we limit the neighborhood of interest to a small portion of the vessel (e.g. the introductory vessel or

either of the bifurcations), we can see that the flow is fairly uniform over the area. This is similar to the mesoscale, or material behavior. The behavior is locally uniform even if globally heterogeneous. If we further reduce our neighborhood to a nearly molecular level, the molecular motion is highly degenerate and rarely in the direction of the bulk or average flow. This neighborhood is representative of the constituent scale—on the order of constituents that are combined to make material. Despite the fact that the behavior is different between the constituents (each of the individual fluid particles has vastly different motion), if we integrate the behavior of all of these constituents over a volume large enough to include molecules that span the range of possibilities, we get a representation of the local blood flow—i.e., the flow for a region large enough to include degeneracies of constituents yet small enough to avoid global heterogeneities.

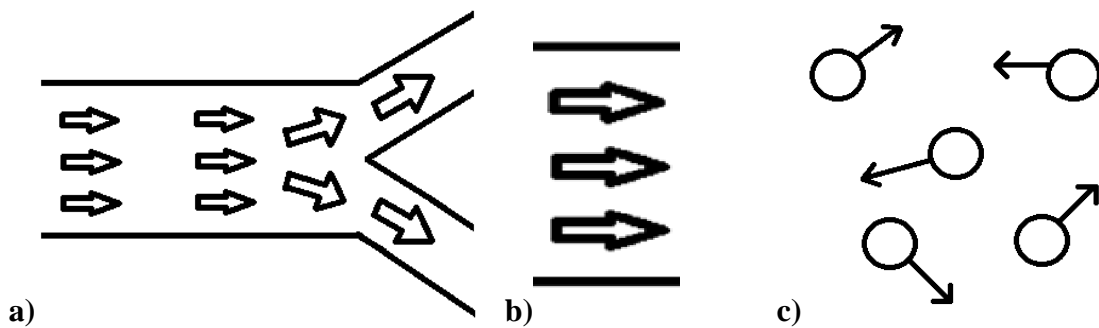


**Figure 1: Graphical Representation of Length Scales of Interest.** Flow of a fluid through a vessel with a bifurcation at a) the body scale, b) the mesoscale, and c) the constituent scale (representation of a molecular component of the fluid)

### *2.3 Variation and Uniformity*

In order to further clarify the concept of the mesoscale I offer the ideas of variation and uniformity. Variation is the relative change in behavior across a neighborhood of interest and its inverse is defined as uniformity. When we look at the entirety of the vessel, we see that there is a high degree of variation in the flow through the introductory vessels and bifurcation and, conversely, a low degree of uniformity. When we narrow the neighborhood of interest to that of the material scale, variation reaches a minimum and uniformity, a maximum – the flow appears to be entirely aimed in one, uniform direction. If we, once again, narrow the neighborhood to the particle level, we see that the degree of variation between the directions of flow of each of the constituents has increased substantially and the degree of uniformity has decreased.

In essence, I have defined the mesoscale as the scale in which the uniformity of the behavior is greatest and the variation is smallest (See Figure 2). This level is the only scale at which the material behavior (constitutive behavior) can be uniquely defined because it is the only scale that is large enough that we can integrate over the degeneracies in constituent behavior yet small enough that it is independent of the body geometry or body scale heterogeneities.

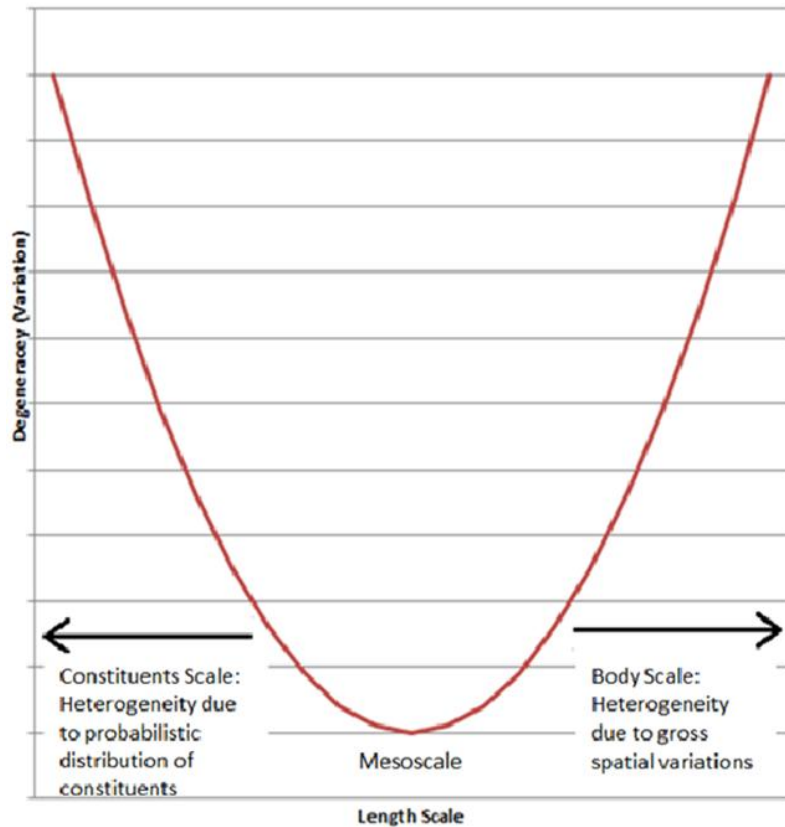


**Figure 2: Degeneracy Plot across Length Scales.**

#### *2.4 Uniqueness and Completeness*

With this definition of the mesoscale, let us define “uniqueness” and “completeness” in the context of material modeling or constitutive modeling. Given a constitutive framework for representing material behavior, uniqueness is assured if the framework is invertible, or one-to-one. This means that for every possible set of parameters of the model, there is one behavior that is associated with it. Additionally, for every behavior that abides by material class restrictions, there is one set of parameters that represents it. Given a constitutive framework, completeness is assured if there is at

least one representation for every possible behavior that fits all assumptions made in developing the model.

A common aspect of many mechanistic models is to incorporate micro- or nanoscale terms together with mesoscale terms—e.g., utilizing a fiber distribution function (micro scale term) together with a bulk isotropic response for the matrix (meso-scale term). This method of formulating a model leads to a characteristic I call “mixed formulation” as the model mathematically mixes two or more scales, specifically having terms representing the constituents and the constitutive. Given the degeneracies at the constituent scale, if a model incorporates a separate constituent term, it is adding variation that should not be present if uniqueness is to be optimal at the mesoscale. In essence, the inclusion of constituents makes the determination of material behavior a multi-body problem — i.e. each constituent is a body and the tissue is composed of multiple bodies. Such complexity is surely necessary to determine molecular mechanisms for material behavior but such n-body complexities prevent the possibility of uniqueness in material behavior — a necessary condition for inverse solutions.



### 3. CRITICAL EVALUATION OF MECHANISTIC MODELS

#### *3.1 Literature Search and Analysis*

In order to determine current trends in mechanistic models and their potential for use in mesoscale modeling, several articles by different authors were evaluated. The main means of finding these papers was to search key terms including “constitutive, mechanistic, multiscale, model,” among others, into the Science Direct search feature. After finding multiple articles, additional papers were found by identifying additional models through references listed in the initial “seed” papers.

From over forty articles found, seventeen were selected for further analysis (See Table 2). The selected papers were chosen for the wide applicability and potential for use amongst them as well as to account for the models developed by differing authors or for different applications.

The articles, and the models contained within, were examined to determine the characteristics of the models, most especially in regards to uniqueness. The constitutive relations were categorized as:

- Unique – for every behavior there is one representation and vice versa
- Incomplete – cannot fully characterize all possible material behaviors that abide by material class assumptions
- Ill-Conceived – choice of principal invariants magnifies measurement error unnecessarily or there is an infinite degeneracy due to the use of six strain measures for incompressible material (only 5 are independent).

- Mixed Formulation – makes the determination of material behavior a multi-body problem, and/or mixes the meso and micro scales such that the meso scale response cannot be determined.

The method of discovering academic manuscripts for analysis is the same as that which is used to provide for a more specified analysis of arterial models. It will also be used to determine the definition of a representative volume element and how it compares to the definition of the mesoscale.

### 3.2 Results and Discussion

Model Author (Year Published)	(Location of Mechanistic Model in Text) Characteristics Identified of the Model	Applicable to Mesoscale Modeling?
Balzani et al (2005)	4.2 Stored-energy function ... : Mixed Formulation	No
Criscione et al (2001)	(6.5) Unique, Complete	Yes
Criscione (2004)	(7.1) Unique, Complete	Yes
deBotton et al (2009)	(12) Mixed Formulation, III-Conceived	No
Driessen et al (2003)	(1) Mixed Formulation, Incomplete	No
Gasser et al (2002)	(9) Mixed Formulation, (26) Mixed Formulation	No
Hill et al (2012)	(1) Mixed Formulation, (2) III-Conceived	No
Holzapfel (2000)	(2) Mixed Formulation, Incomplete	No
Holzapfel et al (2001)	(33) Incomplete, (37) III-Conceived, (57) Mixed Formulation	No
Holzapfel, Ogden (2007)	(4) III-Conceived, (5) III-Conceived, (6) III-Conceived	No
Humphrey, Yin (1987)	pg 569: Mixed Formulation	No
Itskov, Aksel (2004)	(68) III-Conceived	No
Kroon, Holzapfel (2008)	(3) Mixed Formulation	No
Limbert (2011)	(39) Incomplete, (49) Mixed Formulation	No
Schroder, Neff (2002)	(3.27) Mixed Formulation, III-Conceived	No
Stalhand et al (2010)	(28) Mixed Formulation, (29) III-Conceived	No
Zulliger et al (2003)	2.4 Strain energy functions ... : Mixed Formulation	No

**Table 2: List of Mechanistic Models with Characterizations.** Lists a variety of mechanistic models, their uniqueness characteristics, and whether or not they can be used to represent mesoscale behavior for the purpose of multi-scale modeling.

Uniqueness, as discussed earlier, is assured only if the representation is one-to-one with behavior. This characteristic is necessary for representations of mesoscale behavior for which further investigations of sub-scale mechanisms are sought. For instance, if the effect of collagen content on tendon behavior is sought, then such a link is impossible if a framework for representing “tendon behavior” itself is degenerate. It is ill-conceived if the framework permits an infinite number of representations for the same behavior—i.e., changes in representation can be arbitrary (or immaterial) and not related to collagen content for this example.

Although many specific representations (i.e., particular forms of strain energy) are non-degenerate, most are, nevertheless, incomplete. Completeness was defined earlier as having at least one representation for every behavior that maintains all assumptions. Therefore, an incomplete model, for example, is one that uses too few principal invariants to fully characterize all possible material behaviors—i.e., the use of  $I_1$  and  $I_4$  to represent incompressible, transversely isotropic behavior when  $I_1$ ,  $I_2$ ,  $I_4$ , and  $I_5$  are needed for completeness. Incomplete models are a restricted formulation of the material behavior and cannot generally characterize the behavior at the mesoscale. In short, when using incomplete models, a large number of materials that satisfy assumptions will be excluded from characterization.

With regard to non-uniqueness, or degeneracy in representation, two types are identified herein. Mixed formulation means two scales are mixed together in the representation. Ill-conceived means that the strain parameters (i.e., principal invariants or strain components) that are utilized to express the constitutive relation, in turn make

the representation degenerate (or too nearly so such that invertability is impossible in practice due to magnification of measurement error).

The first of these is the most common for the models listed: the utilization of micro-scale parameters in a meso-scale model. These models represent their strain energy function as a sum of the physical behaviors from two or more scales. Because individual elements, like fibers, are on the constituent scale or micro-scale, a mixed formulation is not a mesoscale model per se. A mixed scale model may fit data; however, degeneracy is unavoidable when summing up micro-scale elements, as there are an infinity of micro-scale combinations with the same mesoscale summation. More importantly, a micro-scale integration for representing a mesoscale model simply states that yellow + blue = yellow + blue and loses the concept of what it means to be “green” (i.e. yellow + blue = green). The point here is that the behavior at the material scale is a different entity than the behavior at the constituent scale and that representing a model with a term describing constituent behavior does not account or provide for this difference and mesoscale behavior remains wanting (see Criscione 2008, 2011).

The second characteristic that makes a model inapplicable to multiscale modeling is a model that is ill-conceived for inverse problems. The most common reason that a model is ill-conceived is due to a high co-alignment between the principal invariants used to develop the model. This co-alignment leads to the magnification of measurement error to very large degrees. The co-alignment ratio  $R_C$  of two tensors, as defined in Criscione 2002, 2003 (see covariance ratio), is the absolute value of their inner product divided by their magnitude. Mathematically it is represented as:

$$R_C = \frac{\text{abs}(A_1 \cdot A_2)}{|A_1||A_2|} \quad (3.2.1)$$

For instance, if we let the principal invariants  $I_1$  and  $I_2$  be such that  $\frac{\delta I_1}{\delta F}$  is how  $I_1$  depends on  $F$  and  $\frac{\delta I_2}{\delta F}$  is how  $I_2$  depends on  $F$ , these principal invariants are highly co-aligned. Regarding the equation, it can be seen that the highest co-alignment will occur when the invariant responses are collinear whereas the least co-alignment (i.e., zero) is when they are mutually orthogonal. Perfect co-alignment of principle invariants makes a model non-unique; however, the more co-aligned the principal invariants are, the greater the magnification of measurement error. This error will propagate through all subsequent calculations and the error will be magnified by a factor of  $(1 - R_C(A_1, A_2)^2)^{-1/2}$  (Criscione 2003). This increased error effectively makes the model indeterminable. In this sense, although models using principle invariants  $I_1$  and  $I_2$  can be seen as unique, the measurement error makes them practically non-unique—i.e., large variations in model parameters are associated with small, unmeasurable changes in behavior. Lastly, the popular “Fung elastic” model is one that is within a class of functions that are non-unique. Any function of the form  $W(E_{11}, E_{22}, E_{33}, E_{12}, E_{23}, E_{31})$  for incompressible models is non-unique because the six strain components cannot be varied independently of each other, making them perfectly co-aligned. Consult Criscione (2002, 2003, 2008) for a more detailed discussion of co-alignment.

Determining the constitutive behavior of biological tissues is experimentally challenging, and just fitting test data with a model is a significant achievement that has

great utility for many applications. Nevertheless, when a link is sought between meso-scale (tissue) behavior and micro-scale (cells, fibers, etc) behavior, fitting data is insufficient because tissue behavior needs to be determinable. For data fitting, any forward solution can be used, whereas for behavior to be determinable, uniqueness needs to be established *a priori*. Except for the works by Criscione, which make determinability a defining aspect of model development, all other representations found were unsuitable for multiscale modeling because they were ill-conceived, incomplete, and / or a mixture of meso and micro scale parameters.

## **4. CRITICAL REVIEW SPECIFIED TO ARTERIAL MODELS**

### *4.1 Introduction*

In order to clearly define the means by which the models included herein are characterized (i.e. Incomplete, Ill-Conceived, Mixed-Formulation, etc.), I selected an additional 5 models more specifically applied to vasculature to characterize. The models were found by the same manner as those of Section 3 but were more critically selected for their approach to vasculature. These models and their characterizations can be found in Table 3. I wanted to make fully clear the process by which these models were labeled and so, for each of the 5 models, I give a brief description of the model, present the model in its entirety, and then detail the analysis of the model leading to its characterization. Once again, it should be clarified that all of the models discussed can fit the data used to develop them and that utilizing the model to this end is a valid and substantial aim. However, with regards to applying the model to multiscale modeling, none of the models presented below have the requisite characteristics of uniqueness and completeness.

Model Author (Year Published)	(Location of Mechanistic Model in Text) Characteristics Identified of the Model	Applicable to Mesoscale Modeling?
Delfino et al (1997)	(1): Incomplete	No
Holzapfel, Gasser, Stadler (2002)	(15): Incomplete	No
Horgan, Saccomandi (2003)	(77-78): Mixed Formulation, Overexpressed/Incomplete, III-Conceived	No
Pena et al. (2010)	(3-7): Mixed Formulation, Incomplete	No
Zulliger et al. (2004)	(27): Mixed Formulation, Incomplete	No

**Table 3: List of Arterial Mechanics Models with Characterizations.** Lists several mechanistic models specifically tailored for vascular wall mechanics, their uniqueness characteristics, and whether or not they can be applied to multiscale modeling.

#### 4.2 Delfino et al. (1997)

In a paper entitled “Residual strain effects on the stress field in a thick wall finite element model of the human carotid bifurcation,” Delfino et al. wish to add the effects of residual strain to a finite element model of a bifurcation in a carotid artery. In order to do this, they present a strain energy function that characterizes an artery assumed to be a thick-walled tube made of incompressible, isotropic, and homogeneous material. The strain energy function they use is given by:

$$W = \frac{a}{b} \left[ \exp\left(\frac{b}{2}(I_1 - 3)\right) - 1 \right] \quad (4.2)$$

where  $I_1$  is the first principal invariant of the strain tensor and  $a$  and  $b$  are material constants. The first principal invariant,  $I_1$ , is the trace of the strain tensor,  $\sigma$  and represents volumetric strain in the artery. However, simply defining the strain energy in terms of  $I_1$  eliminates a large number of material behaviors from consideration. In order



to fully characterize all potential behaviors and materials, additional invariants are needed. Therefore, this strain energy function is considered incomplete as it cannot provide a one-to-one relationship between representation and behavior; there are materials that satisfy all assumptions but are excluded from characterization due to too few principal invariants. This incompleteness also eliminates the model from consideration for multiscale modeling.

#### 4.3 Holzapfel, Gasser, Stadler (2002)

The next model considered was presented by Holzapfel, Gasser, and Stadler in a 2002 paper: “A structural model for the viscoelastic behavior of arterial walls: Continuum formulation and finite element analysis.” The authors make the assumptions that the artery is an incompressible, elastic, two-layer fiber-reinforced composite. They consider the two layers to be modeled the media, M, and the adventitia, A. They propose particularizations of the strain energy function for each of these two layers, which only differ in the set of material parameters used. The strain energy functions for the media and adventitia respectively are:

$$\psi_M = \frac{c_M}{2} (I_1 - 3) + \frac{k_{1M}}{2k_{2M}} \sum_{i=4,6} \{ \exp[k_{2M} (I_{iM} - 1)^2] - 1 \} \quad (4.3.1)$$

$$\psi_A = \frac{c_A}{2} (I_1 - 3) + \frac{k_{1A}}{2k_{2A}} \sum_{i=4,6} \{ \exp[k_{2A} (I_{iA} - 1)^2] - 1 \} \quad (4.3.2)$$

Where  $c_M$ ,  $k_{1M}$ ,  $k_{2M}$  and  $c_A$ ,  $k_{1A}$ ,  $k_{2A}$  are the material parameters associated with the media and adventitia. Separating the strain energy function in this way, one for each of

the layers, does not preclude it from uniqueness; however, its lack of principal invariants effectively does. In each of these particular functions, only  $I_1$ ,  $I_4$ , and  $I_6$  are considered where  $I_1$  characterizes the volumetric stress and  $I_4$  and  $I_6$  are defined as the squares of the stretches in the two families of fibers. Once again, as in the Delfino paper, this is too few invariants to fully characterize all possible material behaviors given the assumptions. Therefore this model is also incomplete and, subsequently, not applicable to multiscale modeling.

#### 4.4 Horgan, Saccomandi (2003)

In the 2003 paper “A description of arterial wall mechanics using limiting chain extensibility constitutive models,” Horgan and Saccomandi present a model that is an adaptation of a model proposed by Gent in 1996. The model they present is to be used to characterize an anisotropic, incompressible, elastic solid with two preferred directions which could be due to fiber reinforcement. The adapted model first breaks the strain energy function in the following manner:

$$W = W_{ISO}(I_1, I) + W_{ANISO}(I_4, I_5, I_6, I_7, I_8) \quad (4.4.1)$$

where  $I_1$  and  $I_{4-8}$  are the first and fourth through eighth principal invariants respectively and  $I$  is an invariant to describe the relationship between the two preferred directions. Breaking up the strain energy function in this manner highlights several non-unique characteristics. The first is that the separation of isotropic and anisotropic behaviors necessitates a mixing of meso and micro scales in order to characterize mesoscale behavior. Therefore, this model is characterized as “mixed formulation.” Additionally, a

set of 7 invariants are used when, for this behavior, only 5 non-co-aligned invariants are needed to fully characterize the behavior. Therefore, the function is overexpressed and leads to several representations for a single behavior, indicating that the function is not one-to-one. The last issue with this particular separation is that the anisotropic term is a function of  $I_4$ ,  $I_5$ ,  $I_6$ , and  $I_7$ . Due to the nature of these principal invariants,  $I_4$  and  $I_5$  are highly co-aligned, as are  $I_6$  and  $I_7$ . Therefore, although not explicitly making the formulation incomplete, having such co-aligned invariants will magnify errors that will propagate through all subsequent calculations making the model effectively indeterminable. Therefore this particular separation is also ill-conceived due to the poor choice of principal invariants.

The paper goes on to claim that a substitution for the first term in (4.4.1) and a reduction in the number of principal invariants considered would yield a strain energy function of the form:

$$W = \mu \left\{ -\frac{1}{2} (J_{m0} + J_{m1} I) \ln \left( 1 - \frac{I_1 - 3}{J_{m0} + J_{m1} I} \right) + \gamma_1 f^{(1)}(I_4) + \gamma_2 f^{(2)}(I_6) \right\} \quad (4.4.2)$$

where  $\mu$  is the shear modulus,  $J_{m0}$  and  $J_{m1}$  are the constant limiting value for  $(I_1 - 3)$  for each of the fiber directions,  $\gamma_1$  and  $\gamma_2$  are material constants, and  $f^{(1)}$  and  $f^{(2)}$  are the functions characterizing the additional reinforcement in each of the fibers' directions. This expression of the strain energy function suffers from the opposite issue as (4.4.1) in that this representation is lacking in principal invariants and is therefore under expressed. Once again, there are materials that fit the assumptions but will not have their behavior

represented by the function. Using just  $I, I_1, I_4,$  and  $I_6$  when 5 invariants are needed leads to incompleteness and prevents the model from application to multiscale modeling.

#### 4.5 *Pena et al. (2010)*

The model proposed by Pena et al. in “A constitutive formulation of vascular tissue mechanics including viscoelasticity and softening behavior” published in 2010 considers an artery as an anisotropic, incompressible, elastic tube with fibers along two preferential directions. The authors first separate the volumetric and isochoric terms of the strain energy function. This separation does not make the model non-unique; however, further separating the isochoric term into isotropic and anisotropic terms does, as discussed earlier, accounting for the “mixed formulation” characterization. Their model is then broken up further into several different terms as shown below:

$$\Psi = \Psi_{vol}(J) + \Psi_{iso}(I_1) + \Psi_{ani}(I_4, I_6) \quad (4.5.1)$$

where:

$$\begin{aligned} \Psi_{vol} &= \frac{1}{D} [J - 1]^2 & \Psi_{iso} &= [1 - D_m] \Psi_m^0 - \frac{1}{2} \sum_{i=1}^n [C : Q_m^i] \\ \Psi_{ani} &= [1 - D_{f1}] \Psi_{f1}^0 + [1 - D_{f2}] \Psi_{f2}^0 - \frac{1}{2} \sum_{i=1}^n [C : Q_{f1}^i + C : Q_{f2}^i] \end{aligned} \quad (4.5.2)_{1-3}$$

where  $J$  is the determinant of the deformation gradient tensor,  $D_m$  is a variable expressing damage associated with  $I_1$ ,  $D_{f1}$  and  $D_{f2}$  are the damage variables associated with the two fibers,  $Q_m$  is a tensor expressing the elastic response of the material associated with  $I_1$ , and  $Q_{f1}$  and  $Q_{f2}$  are stress tensor expressing the direction elastic

response associated with the fiber directions and the related invariants,  $I_4$  and  $I_6$  respectively. Additionally,

$$\begin{aligned}\Psi_m^0 &= \mu[I_1 - 3], & \Psi_{f1}^0 &= \frac{k_1}{2k_2} [\exp(k_2[I_4 - 1]^2) - 1], \\ \Psi_{f2}^0 &= \frac{k_3}{2k_4} [\exp(k_{42}[I_{64} - 1]^2) - 1]\end{aligned}\tag{4.5.3}_{1-3}$$

where  $\mu$  is a stress-like constant,  $k_1$  and  $k_3$  are stress-valued constants, and  $k_2$  and  $k_4$  are dimensionless constants. Putting this all together shows that the strain energy function ends up being solely in terms of  $I_1$ ,  $I_4$ , and  $I_6$  thereby making the formulation incomplete for the same reasons as many of the other models presented herein.

#### 4.6 Zulliger et al. (2004)

The final model to be considered is one presented by Zulliger et al. in “A strain energy function for arteries accounting for wall composition and structure,” published in 2004. For this model, they assume the artery to be elastic, incompressible, and double fiber-reinforced (collagen and elastin). The authors, like several of the others already presented, separate the strain energy function in to isotropic and anisotropic terms. Separating the strain energy function into these components, as with the others, leads to the “mixed formulation” characterization for the formulation and its non-uniqueness. They then characterize each of separated terms with functions relating that component of the strain energy function to collagen and elastin fractions. The final model is then summed to be:

$$\Psi = f_{elast} c_{elast} (I_1 - 3)^{3/2} + f_{coll} \left( \frac{1}{2} \Psi_{coll}(\sqrt{I_4} - 1) + \frac{1}{2} \Psi_{coll}(\sqrt{I_{4'}} - 1) \right) \quad (4.6)$$

where  $f_{elast}$  and  $f_{coll}$  are the fractions of elastin and collagen, respectively,  $\Psi_{elast}$  and  $\Psi_{coll}$  are the strain energy functions representing the mechanical properties of elastin and collagen, respectively,  $I_1$  is the trace of the Cauchy-Green deformation tensor,  $C$ ,  $I_4$  is the principal invariant characterizing the first fiber's preferential direction, and  $I_{4'}$  characterizes the second fiber's preferential direction (often seen as  $I_6$ ). It should be readily apparent by now that, in addition to its “mixed formulation” characterization, this model is incomplete due to a lack of principal invariants. The model is only in terms of  $I_1$ ,  $I_4$ , and  $I_6$  and is, therefore, incomplete and cannot be used for multiscale modeling.

#### 4.7 Conclusion

Providing an in-depth analysis of the models and the reasons behind the characterizations determined for each allows for a better understanding of some of the features of mechanistic models that make them inapplicable to multiscale modeling. Therefore, future models, if a potential aim might be an application to multiscale modeling, might take the features into account in the development of the models. It is also worth noting that for many of the models utilizing the usual set of principal invariants ( $I_{1-7}$ ), if the models were determined to be complete (i.e. they utilize the necessary 5 invariants to characterize incompressible material behavior) the likelihood that the models would then be ill-conceived is high due to the high degree of co-alignment between many of the invariants. This would dramatically increase the effects

of measurement error to the point that the model would effectively be indeterminable. Therefore, the strain energy function needs to be established with a better set of invariants to minimize the co-alignment between, like those used by Criscione (2001, 2004).

## 5. MESOSCALE AND THE REPRESENTATIVE VOLUME ELEMENT

### *5.1 Defining the Representative Volume Element*

During the search for a definition of the mesoscale that was well-suited for multiscale modeling, I came across the term representative volume element (or RVE) used commonly in biomaterials. Not finding a definition for the mesoscale well-suited for the aim of multiscale modeling, an alternative definition was provided herein. However, due to their similarity, it would be helpful to expound upon how these terms compare.

The first expression of *representative volume element* that I was able to find was in a 1963 paper by Hill (Hill 1963). In this paper, he stated that “this phrase will be used when referring to a sample that (a) is structurally entirely typical of the whole mixture on average, and (b) contains a sufficient number of inclusions for the apparent overall moduli to be effectively independent of the surface values of traction and displacement, so long as these values are macroscopically uniform.” The first part of this definition is a statement concerning the statistics of the material and the selected volume—that the selected volume must contain enough of the composite’s microheterogeneities (i.e. grains, inclusions, voids, cracks, fibers, etc.) to be statistically representative of the composite as a whole. The second part of the definition states that the RVE must be wholly independent of the forces applied to the surface of the composite. This second aspect necessitates that rigorous boundary conditions be applied to the selected volume so that its behavior best simulates the actual deformation within the composite.



Depending on which assumptions are made, varying values of material parameters may be attained for the same representative sample. For instance, if strain were assumed to be constant throughout the composite this would lead to a Voigt estimate of the parameter (as Voigt first proposed the assumption). Alternatively, if stress were assumed to be uniform throughout the composite, the parameter would be estimated by a Reuss estimate. These estimates represent the upper and lower bounds, respectively, of the material parameters for the selected volume (Hill 1963). These material parameters are dependent on constituent parameters like volume fraction, size, and distance between constituents all of which are statistically represented by the volume selected as the RVE. Because all of these factors are volumetrically dependent, the moduli and behavior of the composite can then be found by summing across all the RVE's contained within the composite.

However, there are two other well-known and accepted definitions for the RVE, one by Drugan and Willis and the other by Kanit et al. Drugan and Willis state that the Hill interpretation of the RVE is qualitative in its approach and that the RVE must be chosen "sufficiently large" compared to the size of constituents in order to be statistically representative of all of the composite's microheterogeneities and therefore, to be valid. They therefore propose that the RVE be "the smallest material volume of the composite for which the usual spatially constant overall modulus macroscopic constitutive representation is a sufficiently accurate model to represent mean constitutive response" (Drugan and Willis 1996). This varies from Hill's definition as Hill's aims to determine the parameters of the composite from those of a selected statistically

representative volume. Drugan and Willis', however, aims to determine the smallest volume at which the material parameters match, to a sufficient degree, those of the whole composite. This definition for the RVE has a significantly differing aim from both Hill's definition and the definition for the mesoscale described in this paper and, thus, this will be the last mention of it herein. Kanit et al. state that this definition does not take into account statistical variations of the material parameters across finite domains. They, therefore, offer another definition: that "the RVE must ensure a given accuracy of the estimated property obtained by spatial averaging of the stress, strain, or the energy fields in a given domain  $V$ ." They go on to say that if smaller volumes are considered, averages must be taken over several values in order to get the same accuracy, if bias is not introduced by edge effects due to boundary conditions. Their definition, then, aims to take the variations of material parameters into account and the size of the RVE then depends on the particular property being investigated.

## *5.2 Comparing RVE and the Mesoscale*

Now that a detailed description of RVE has been provided, I can compare this concept with that of the mesoscale provided in this paper. The definition for the mesoscale in this paper takes some aspects of Hill's definition for the RVE and builds upon them. The primary similarity is that for both terms, the volume of interest, termed neighborhood for the mesoscale, must be statistically representative in that they must contain all constituents and in appropriate number that they are wholly characteristic of the entire body. This allows the averaging across the neighborhoods to

determine the overall body behavior. Comparing to Kanit et al.'s definition of the RVE, the mesoscale also takes into account the variations in material parameters as it is characterized by a minimization in the variation within the neighborhood of interest. The mesoscale, then, encompasses certain characteristics of both Hill and Kanit et al.'s definitions for the RVE. However, the RVE's size is determined by restrictive boundary conditions and assumptions whereas the mesoscale's size is determined by minimizing the variation and maximizing the uniformity of the area of interest.

Another difference between the definitions for the RVE and the mesoscale is that the RVE's across the composite are considered identical and will therefore exhibit identical stress and strain fields (Sun and Vaidya 1996). Alternatively, the mesoscale neighborhoods, although having a minimized variation within, may vary from each other according to the body geometry of the macroscale.

A last point must be made here as it concerns a definition for the mesoscale differing from that presented earlier and intimately related to the RVE. Ostoja-Starzewski, in a 2002 paper, denotes the scale of the microstructures as  $d$ , the scale of the macroscopic body as  $L_{macro}$ , and  $L$  as some scale of the material domain, large enough compared to the microscale so that it is independent of body geometry. In order to separate the scales of interest, he defines a term,  $\delta$ , as  $L/d$  and then separates the scales in the following manner:  $\delta < \infty$  is considered the mesoscale,  $\delta \rightarrow \infty$  is considered the macroscale, and  $\delta \approx 1$  is considered the microscale (Ostaja-Starzewski, 2002). This characterization of the scales of interest is very different from that provided earlier. The mesoscale defined in this paper ensures a statistical representation of the material body

and that variation within is at a minimum. Contrasted, the separation of scales provided by Ostoja-Starzewski does not take these factors into consideration, nor does it account for the variation in material parameters. For these reasons, the separation of scales defined in Section 2 is more suited for multiscale modeling than that provided by Ostoja-Starzewski.

Therefore, although the terms for the mesoscale and representative volume element are similar, there are some clear differences. The differences outlined in this section are evidence that a new definition for the mesoscale, tailored for multiscale modeling, was needed. Some elements of the RVE, which is mostly used in biomaterials, are similar to those of the mesoscale defined herein. However, the mesoscale builds on many of these elements and makes it well-suited for multiscale modeling.

## 6. ENERGY FUNCTION FIT TO SHEEP AORT INFLATION DATA

### 6.1 Method of Data Collection

I was given two lengths of sheep aorta to be used for mechanical testing and analysis. The aortas were suspended in a phosphate buffered solution (PBS) and kept cool in a refrigerator. I cut 5 shortened lengths from the aortas and stretched their axial length to approximately 110% of their original lengths. This was done by suturing toothpicks along the length of the aorta but the sutures were separated by a length 10% longer than that of the aorta, thereby stretching it. This provided the aorta with axial stretch and strain characteristics analogous to the behavior that would be seen in a functioning aorta. Stretching the aorta in this manner allows a focus on how radial stretch affects the behavior of the aorta *in vivo*.

Using a hand-made bladder apparatus with a pressure sensor and a means of filling the bladder, the original volume was found by expanding the bladder inside the aorta by injecting water until the pressure was non-zero. The volume of the bladder at the point at which the pressure became non-zero was logged as the original volume. 1mL boluses of water were then injected steadily into the bladder and the pressure and volume were recorded. The bladder apparatus was used so that it was not necessary for the vertebrals coming off the aorta to be sutured closed, the bladder applied the pressure to the interior of the aorta without exposing the aorta, itself, to any fluid. The bladder was made to be larger in radius than the aorta when fully expanded in order to ensure that it would not bear any of the load due to the its inflation. Therefore, it was assured

that the pressure read was due solely to the wall of the aorta. The pressure data from the pressure sensor was read and interpreted by a Labview program which then established a plot for Pressure vs. Time. The point at which the pressure plateaued post bolus injection, the steady-state pressure, was logged as the pressure for that particular volume. In this way, the volume was steadily increased and the corresponding pressures were recorded. The volume was increased until the pressure within the aorta approached 140mm Hg at which point the test was ended to protect the aorta for future testing. This sequence was performed three times for each aorta. The pressure/volume data points for all tests were then used collectively for subsequent calculations.

## 6.2 Constitutive Framework

The constitutive framework used to develop the model was that presented by Criscione in 2004 (Criscione 2004). The six principal invariants used, as opposed to the more commonly used  $I_{1-7}$ , were Criscione's stretch-like parameters  $\gamma_{1-6}$ .  $\mathbf{F}$  is defined as the deformation gradient and  $\mathbf{R}$ ,  $\mathbf{Q}$ , and  $\mathbf{Z}$  are defined as unit vectors corresponding to the radial, circumferential, and axial directions of a cylindrical coordinate system in a strain-free state, respectively. Similarly,  $\mathbf{r}$ ,  $\mathbf{q}$ , and  $\mathbf{z}$  represent the radial, circumferential, and axial directions in the current, or strained, state. With these terms defined, the six scalar strain attributes are:

$$\begin{aligned} \gamma_1 &= \ln(J), & \gamma_2 &= \frac{3}{2} \ln(\lambda_Z), & \gamma_3 &= 2 \ln \zeta, \\ \gamma_4 &= \Phi_{ZR}, & \gamma_5 &= \Phi_{QZ}, & \gamma_6 &= \Phi_{QR} \end{aligned} \quad (6.2.1)_{1-6}$$

where:

$$J = \det(\mathbf{F}), \quad \zeta = J^{-1/3} \lambda_z^{1/2} (\mathbf{q} \cdot \mathbf{FQ}). \quad (6.2.2)_{1-2}$$

$\phi_{ZR}$  is the ratio of Z displacement increment with R increment,  $\phi_{QZ}$  is the ratio of hoop displacement increment with Z increment, and  $\phi_{QR}$  is the ratio of hoop displacement increment with R increment. Each of these six strain attributes has a physical interpretation and each is associated with a particular type of deformation. By carefully applying strains to a straight axis-symmetric tube, one can produce deformations in which just one of the six attributes is non-zero, providing useful physical interpretations.

1.  $\gamma_1$  is associated with dilatation strain because for a pure dilatation, the other attributes are zero whereas  $\gamma_1$  will always be  $\ln(J)$ .
2.  $\gamma_2$  is associated with distorted, axial strain. When exposed to uniaxial, isochoric stretch of  $\lambda_z$  in the  $\mathbf{Z}$  direction, the other attributes are zero whereas  $\gamma_2$  is  $\ln(\lambda_z^{3/2})$ .
3.  $\gamma_3$  is associated with luminal inflation because in this instance the hoop direction increases but the wall thins. If the hoop direction increases by the stretch ratio  $\lambda_Q$  then the radial direction will thin by  $\lambda_Q^{-1}$  and the other attributes will be zero whereas  $\gamma_3$  will be  $\ln(\lambda_Q^2)$ .
4.  $\gamma_4$  is associated with axial or telescopic shear – the inner wall is displaced axially relative to the outer wall. For this type of deformation, all other attributes will be zero but  $\gamma_4$  will equal  $\phi_{QR}$ .
5.  $\gamma_5$  is associated with torsion of the tube. For this deformation, all other attributes will be zero but  $\gamma_5$  will equal to  $\phi_{QZ}$ .

6.  $\gamma_6$  is associated with circumferential shear – the inner wall is rotated relative to the outer wall. In this case, all other attributes will be zero whereas  $\gamma_6$  will equal  $\varphi_{QR}$ .

Please consult Criscione (2004) for more information regarding these attributes. Utilizing these attributes, as opposed to the principal invariants  $I_{1-7}$ , allows one to develop a model that has a one-to-one relationship between them and the components of the Right Cauchy-Green deformation tensor. The reason for this is that the model will be characterized in terms of six attributes that can be individually varied allowing for a complete characterization of the behavior. Additionally, the attributes listed have very low co-alignment measures and are mostly orthogonal (14 out of the 15 inner products vanish).

For the purposes of modeling the data collected, the aorta is considered a hyperelastic, incompressible, homogeneous tube. Due to these assumptions,  $\gamma_1 = 0$ , as is the case for all incompressible materials, leaving 5 strain attributes to characterize the behavior of the aorta. Additionally, because the only strain applied to the aorta was that of inflation, neither axial or circumferential shears nor any torsion were applied, all of the attributes listed in (6.2.1)<sub>4-6</sub> are zero. Therefore, the dependence of the strain energy function on  $\gamma_{4-6}$  cannot be determined from this test as the testing is focused only on determining the dependence on the inflation parameter,  $\gamma_3$ . The hoop stretch,  $\lambda_Q$ , is dependent only on the radius and is represented as  $\lambda_Q(R)$  and the axial stretch is represented simply by  $\lambda_Z$ . The attributes for this testing procedure are therefore:



$$\begin{aligned}\gamma_1 &= 0, & \gamma_2 &= \ln(\lambda_Z^{3/2}), & \gamma_3 &= \ln \lambda_Q^2(R) + \ln(\lambda_Z), \\ \gamma_4 &= 0, & \gamma_5 &= 0, & \gamma_6 &= 0.\end{aligned}\tag{6.2.3}_{1-6}$$

Because the aorta was pre-stressed in the  $\mathbf{Z}$  direction to *in vivo* levels and was not stretched further in the testing of the aorta, the length,  $l$ , of the vessel during testing is equal to the length,  $L$ , prior to inflation. Therefore, the ratio of these two parameters,  $\lambda_Z$ , is equal to one. With  $\lambda_Z$  known,  $\gamma_2$  is found to be zero. In this way, the only part of  $W$  or  $W(0, \gamma_3, 0, 0, 0, 0)$ , the strain energy function, that can be determined from this test is that of  $\gamma_3$ , as desired.

Because the material is considered incompressible, the volume of the aorta wall remains constant and therefore:

$$V_{\text{wall}} = v_{\text{wall}} \rightarrow \pi L(R^2 - R_{\text{in}}^2) = \pi L(r^2 - r_{\text{in}}^2)\tag{6.2.4}$$

where the lowercase letters represent the current configuration (the stressed state) and the uppercase letters represent the reference configuration (original state).  $R$  and  $r$  are the radial length to the same, arbitrary point in the wall but in the reference and current configurations respectively and  $L$  is the length of the vessel. It can be shown that (6.2.4) can be manipulated to become (6.2.5), the reason for which will be to ease future substitutions.

$$\left(\frac{r}{R}\right)^2 - 1 = \left[\left(\frac{r_{\text{in}}}{R_{\text{in}}}\right)^2 - 1\right] \left(\frac{R_{\text{in}}}{R}\right)^2\tag{6.2.5}$$

The hoop stretch,  $\lambda_Q(R) = r/R$  can then be substituted into (6.2.5) to give:

$$\lambda_Q(R)^2 - 1 = \left[ \lambda_Q(R_{in})^2 - 1 \right] \left( \frac{R_{in}}{R} \right)^2 \quad (6.2.6)$$

a change of variables is useful here wherein  $\beta(R) = \lambda_z \lambda_Q^2(R) - 1$  where  $\lambda_z = 1$ . Therefore,  $\beta(R) = \lambda_Q^2(R) - 1$  is substituted into (5.2.6) to give:

$$\beta(R) = \beta_{in} \left( \frac{R_{in}}{R} \right)^2 \quad (6.2.7)$$

With this change of variable,  $W(0, 0, \gamma_3, 0, 0, 0)$  can be expressed as  $w(\beta)$ , where  $\beta = \exp(\gamma_3) - 1$ . From this expression, it follows that powers of  $\beta$  are related to powers of  $\beta_{in}$  by:

$$\beta^i = \beta_{in}^i \left( \frac{R_{in}}{R} \right)^{2i} \quad (6.2.8)$$

which becomes useful when we wish to express  $\delta w / \delta \beta$  as a power series:

$$\frac{\delta w}{\delta \beta} = \sum_{i=0}^{\infty} \beta^i B_i \quad (6.2.9)$$

### 6.3 Results

Using the original volume, the volume in the stressed state, and the equation established for  $\beta$ , a plot of Pressure vs. Beta could be produced for each aorta tested.

Then, the power series:

$$P = \sum_{i=0}^{\infty} (\beta_{in})^i P_i \quad (6.3.1)$$

can be estimated by fitting a polynomial to the plot. A polynomial fit was chosen because it is a reasonable estimation for the power series listed above and the only

problem that is invertible, a necessary characteristic for future calculations. A fifth order polynomial fit was specifically chosen because such a fit would minimize measurement error while still ensuring a best fit. The plots of the fifth order polynomial fits for each of the aortas also did not systematically deviate from the data, indicating the quality of the fit. The polynomial fit was forced through the origin (0,0) because when  $\beta=0$  the pressure should also be zero as this represents the original volume. The Pressure vs. Beta plots, along with the fifth order polynomial fits and correlation coefficients can be seen in Figure 3.

Utilizing the polynomial fit,  $P_i$  from (6.3.1) can be found for each of the five terms. When  $P_i$  is known, the corresponding value for  $B_i$  in (6.2.9) can be found by inverting:

$$P_i = \begin{cases} 2B_0 \ln\left(\frac{R_{out}}{R_{in}}\right), & i = 0, \\ \frac{B_i}{i} \left( \left(\frac{R_{out}}{R_{in}}\right)^{2i} - 1 \right), & i \geq 1. \end{cases} \quad (6.3.2)$$

The values for  $P_i$  and the calculated  $B_i$  for each of the five terms and each of the five aortas, in addition to the average  $B_i$  are shown in Table 4.

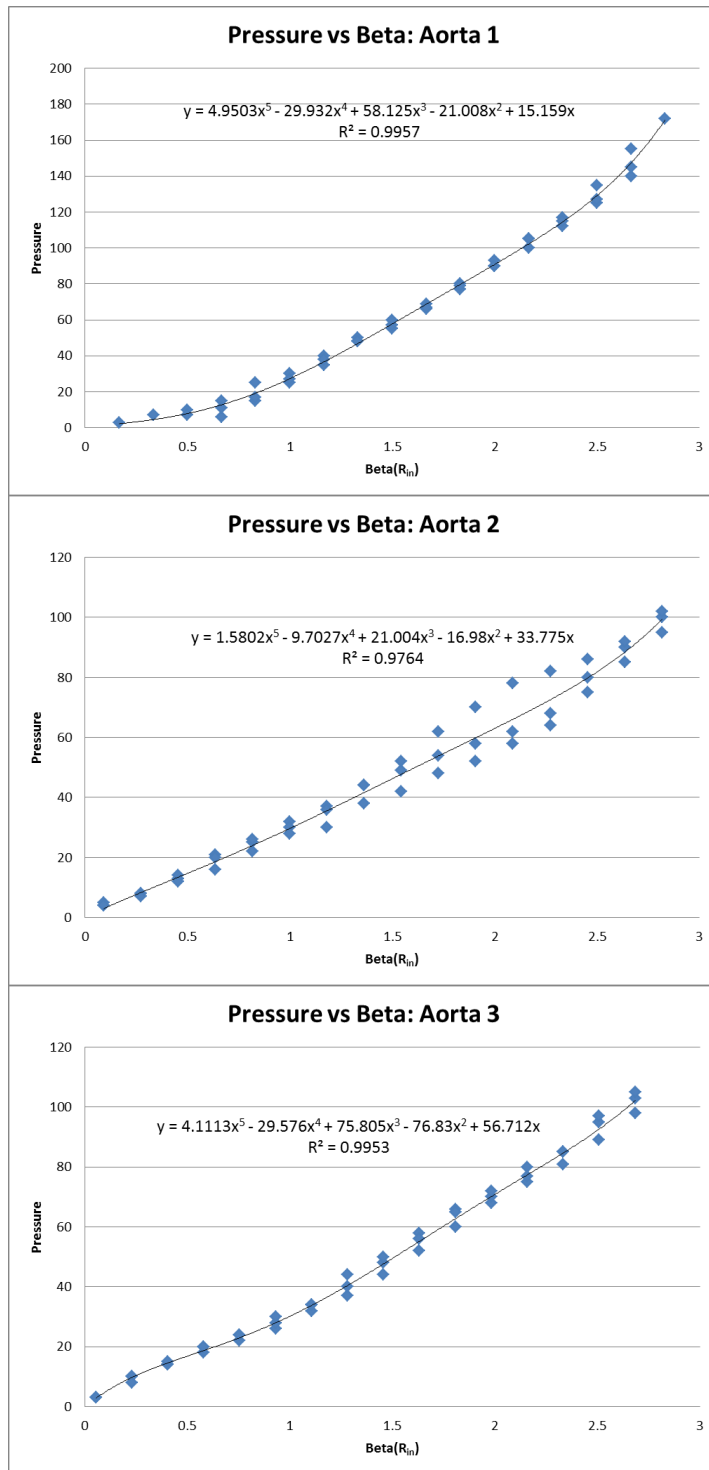


**Figure 3: Pressure vs. Beta for Sheep Aortas Tested in Inflation.** Fifth order polynomial fit and correlation coefficient are shown as well.

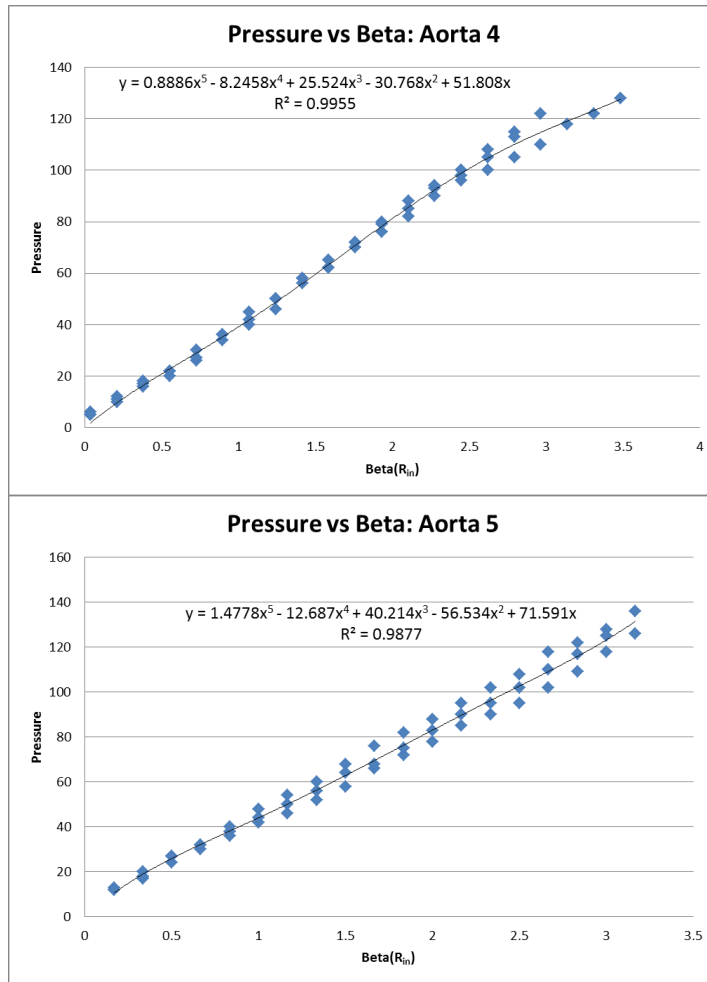


**Figure 3 Continued.**

	Aorta 1		Aorta 2		Aorta 3		Aorta 4		Aorta 5		Average
i	P <sub>i</sub>	B <sub>i</sub>	P <sub>i</sub>	B <sub>i</sub>	P <sub>i</sub>	B <sub>i</sub>	P <sub>i</sub>	B <sub>i</sub>	P <sub>i</sub>	B <sub>i</sub>	B <sub>i</sub>
1	15.16	13.52	33.78	25.54	56.71	47.27	51.81	43.63	71.59	61.52	38.30
2	-21.01	-12.01	-16.98	-7.73	-76.83	-36.05	-30.77	-14.65	-56.53	-27.69	-19.62
3	58.13	20.41	21.00	5.47	75.81	20.54	25.52	7.05	40.21	11.53	13.00
4	-29.93	-6.22	-9.70	-1.38	-29.58	-4.43	-8.25	-1.27	-12.69	-2.04	-3.07
5	4.95	0.59	1.58	0.12	4.11	0.33	0.89	0.07	1.48	0.13	0.25

**Table 4: P<sub>i</sub> and B<sub>i</sub> for Tested Sheep Aortas.** P<sub>i</sub> and B<sub>i</sub> for each of the five terms and each of the five aortas tested as well as the average B<sub>i</sub> for each term are shown.

Using the values shown in Table 4 and equation (6.2.9), an approximation for  $\delta w/\delta\beta$  can be found for each aorta. These approximations can be seen graphically in Figure 4. However, for the sake of space I will only present the equation for the averaged approximation across all five aortas here:

$$\frac{\delta w}{\delta\beta} = 0.25\beta^5 - 3.07\beta^4 + 13.00\beta^3 - 19.62\beta^2 + 38.30\beta . \quad (6.3.3)$$

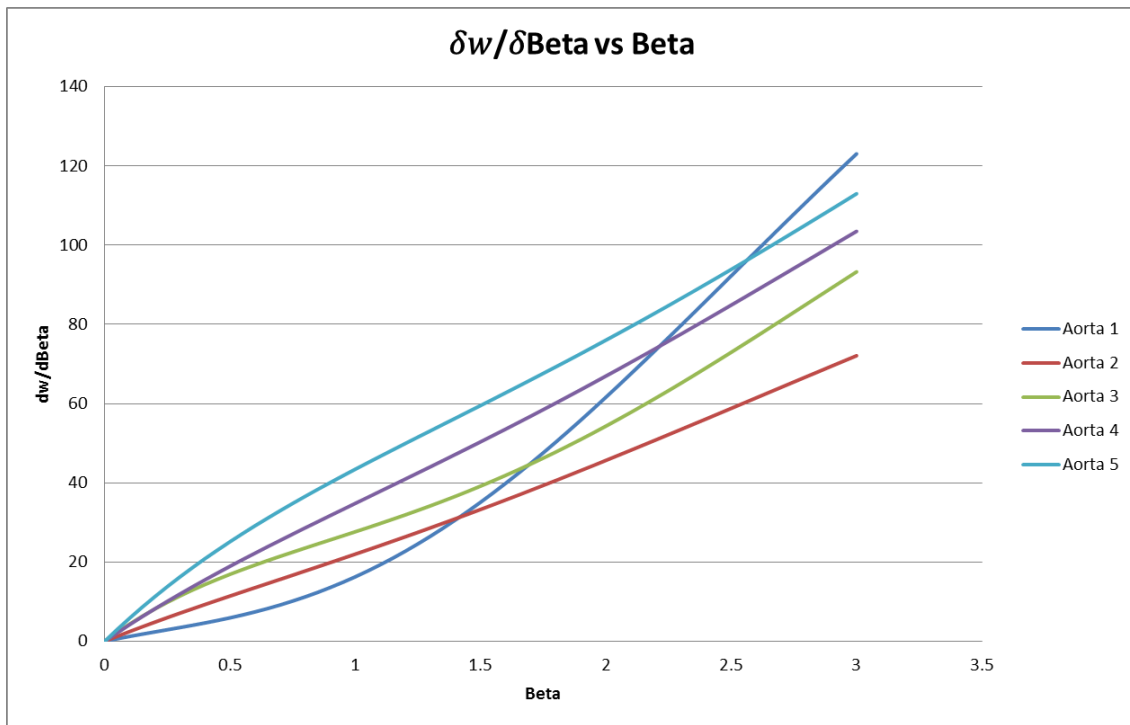


**Figure 4:  $\delta w/\delta\beta$  vs Beta.**

Analyzing Figure 4, one can make the determination that the behavior for Aorta 1 looks markedly different from the others shown. There are potential factors that could be the cause of such differing behavior. The first is that the elasticity of Aorta 1 could be greater over the range when compared to the other aortas. To test this hypothesis, the

physiologic pressure range of 80mmHg – 120 mmHg was specifically considered. The data representing this range of pressures was plotted and linearly fit for each aorta to give an estimation for the comparable elasticity. This can be seen in Figure 5.

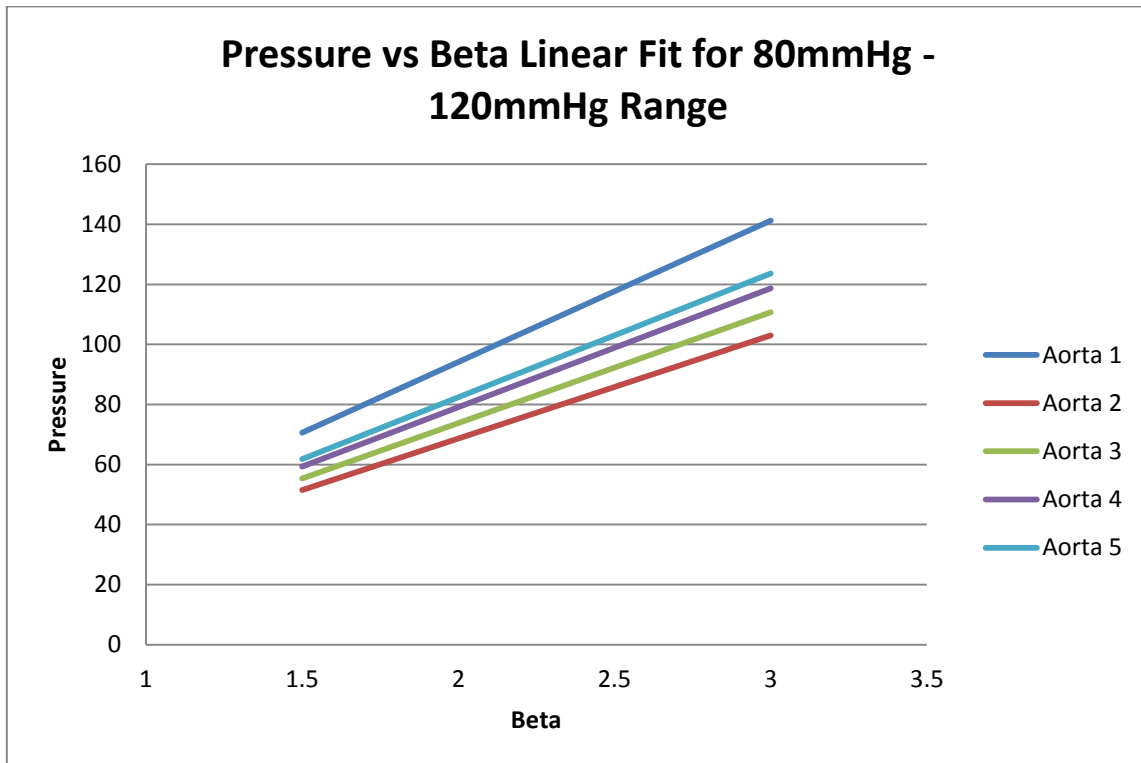


**Figure 5: Pressure vs Beta Fit for 80mmHg – 120mmHg Range.**

The data seems to support this hypothesis as it can be seen that the linear fit for Pressure vs Beta for Aorta 1 is noticeably higher than for any of the other aortas. The fact that it was the first segment cut from its stretch of aorta means that, for the stretch of aorta, it could be either the most proximal or the most distal sample (the direction was not accounted for in the removal of the aortas). Nelson et al. (Nelson et al. 2011) present

data that indicates that the proximal ends of aortas are typically stiffer and more elastic than distal aortas. This seems to support the hypothesis that Aorta 1 was likely the most proximal section as it has been shown to be more elastic than the other samples. This higher elasticity could be the reason for its differing behavior. The other possible explanation is that Aorta 1 was the only aorta tested on that particular date whereas Aortas 2-5 were each tested at a later time. This could indicate a relative decay in the samples over the time period or a potential difference in testing procedure or environment (although attempts were made to prevent this).

In any case, a representation for the strain energy function for inflation in terms of  $\gamma_3$  is sought. Using the chain rule to relate  $W(0, 0, \gamma_3, 0, 0, 0)$  to  $w(\beta)$ , one can show that:

$$\frac{\delta W}{\delta \gamma_3} = \frac{\delta w}{\delta \beta} \exp(\gamma_3) . \quad (6.3.4)$$

Then, substituting each of the  $\frac{\delta w}{\delta \beta}$  representations (i.e. 6.3.3) into (6.3.4), we are able to find how  $W$  depends on  $\gamma_3$ . Again, for the sake of space, only the average representation across all 5 aortas is shown here:

$$\frac{\delta W}{\delta \gamma_3} = \left( 0.25\beta^5 - 3.07\beta^4 + 13.00\beta^3 - 19.62\beta^2 + 38.30\beta \right) \exp(\gamma_3) \quad (6.3.5)$$

where  $\beta = \lambda_Q^2 - 1 = \exp(\gamma_3) - 1$ ,  $\gamma_3 = \ln(\lambda_Q^2)$ , and  $\lambda_Q$  is a stretch ratio describing the deformation in the hoop direction, and its inverse represents the thinning of the wall in the radial direction. However, the representations for  $\frac{\delta W}{\delta \gamma_3}$  for each of the five aortas can be



easily found from Table 4 and equations (6.3.1) and (6.3.4) and are shown, graphically, in Figure 6.

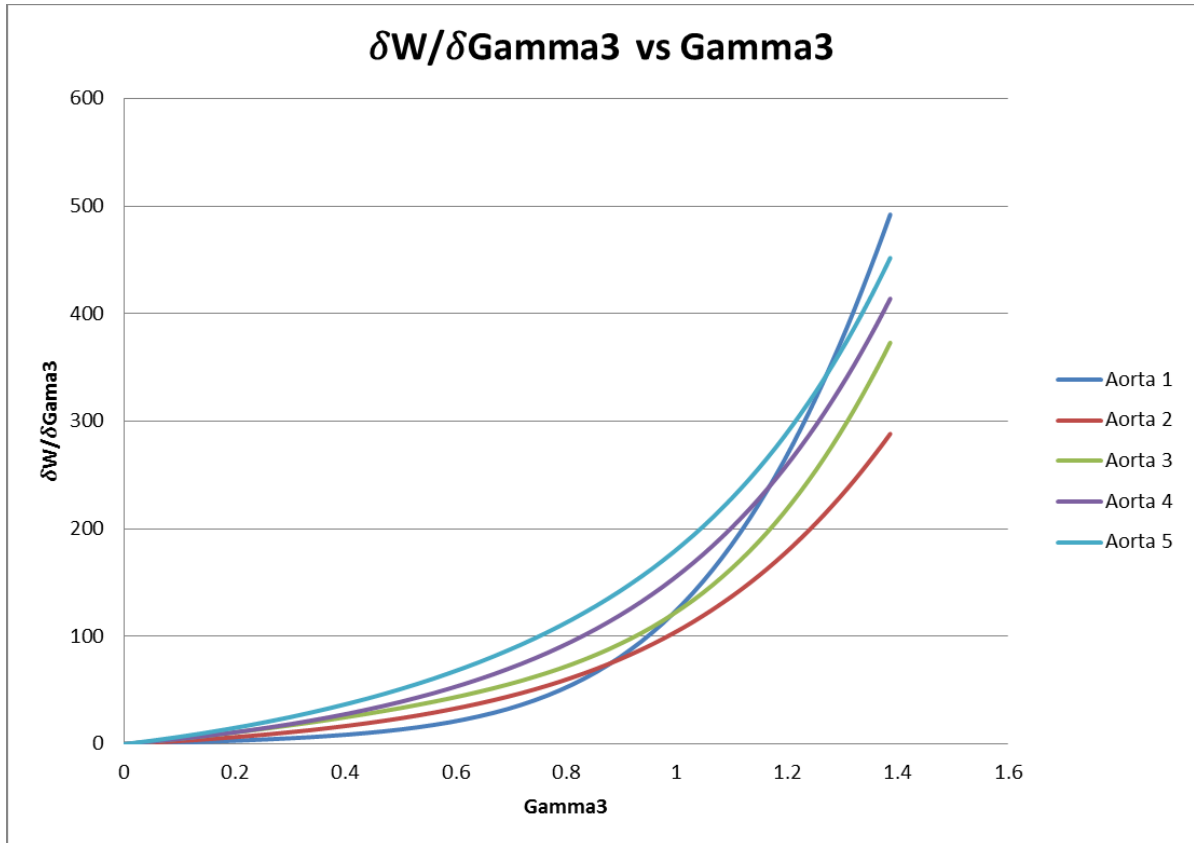


**Figure 6:  $\delta W / \delta \Gamma_3$  vs  $\Gamma_3$ .**

#### 6.4 Concluding Remarks

It should be pointed out that (6.3.5), for inflation strains on hyperelastic, incompressible, homogeneous tubes, is both unique and complete. Unlike many of the other models presented herein, rather than completely neglecting particular principal invariants, I found them to be zero and therefore identified that they would have no effect on the strain energy function under these conditions. Therefore, it was reasonable

to represent the strain energy function as  $W(\gamma_3)$ . However, the model does not represent responses of the aortas to any other types of strain (i.e. shear). For the dependency of the strain energy function under other conditions, additional experiments must be conducted and additional models developed. This is a major benefit of the use of principal invariants  $\gamma_{1-6}$ , as they can be varied independently of each other. Therefore, by similar methods as I found the response under inflation strains, the response to other types of strains can be found utilizing the Criscione framework. In this way, the response to every type of strain and combinations of them can be found and unique and complete models can be developed for each. Because (6.3.5) is both complete and unique for the conditions of interest, it is applicable to multiscale modeling and applying it in this manner is advocated by the author for future work. Additionally, experiments to test the responses to other types of strains in terms of the other  $\gamma$  principal invariants should be devised and conducted to enable the characterization of these behaviors.

## 7. CONCLUSION

It is important to recognize that, although a great deal of effort and research has gone into this thesis, it is but the beginning to the discussion on multiscale modeling that needs to continue in the future. If a truly representative model is sought, one that can represent the tissue behavior across several length scales including the constituent and material scales, uniqueness and completeness must be a defining aspect in the production of the model. These characteristics are a necessity if the model is to be used to “determine” the response of tissue and not simply “fit” it. For this reason, I analyzed several models and determined their applicability to multiscale modeling and identified any features that might limit this aim. I also developed a complete, unique model for inflations strains on a sheep aorta using a constitutive framework outlined by Criscione (Criscione 2004). This particular framework differs from that of the usual framework expressed in terms of the principal invariants  $I_{1-7}$  in that the parameters are nearly all orthogonal and can be varied independently. Future work into mechanistic models for the purposes of multiscale modeling, then, would do well to utilize this framework and to ensure uniqueness and completeness of the model throughout its development. A fully representative model that is both unique and complete and fully characterizes responses to all possible strains could, potentially, be developed utilizing this framework. Such a model could allow for a thorough understanding of tissue behavior, even taking into account the effects of constituent factors.

## REFERENCES

- Balzani D, Neff P, Schröder J, Holzapfel GA. 2006. A polyconvex framework for soft biological tissues. Adjustment to experimental data. *International Journal of Solids and Structures*, **43**: 6052-6070.
- Criscione JC, McCulloch AD, Hunter WC. 2002. Constitutive framework optimized for myocardium and other high-strain, laminar materials with one fiber family. *Journal of the Mechanics and Physics of Solids*, **50**: 1681-1702.
- Criscione JC. 2003. Rivlin's representation formula is ill-conceived for the determination of response functions via biaxial testing. *Journal of Elasticity*, **70**: 129-147.
- Criscione JC. 2004. A constitutive framework for tubular structures that enables a semi-inverse solution to extension and inflation. *Journal of Elasticity*, **77**: 57-81.
- Criscione, John. 2008. Kinematics framework optimized for deformation, growth, and remodeling in vascular organs. *Biomechanics and Modeling in Mechanobiology*, Volume 7, Number 4: 285-293.
- Criscione JC. 2011. On modeling the mechanical behavior of matter: The continuum assumption. *International Journal of Structural Changes in Solids – Mechanics and Applications*, Volume 3, Number 2, pages 55-59.
- deBotton G, Shmuel G. 2009. Mechanics of composites with two families of finitely extensible fibers undergoing large deformations. *Journal of the Mechanics and Physics of Solids*, **57**: 1165-1181.
- Delfino A, Stergiopoulos N, Moore JE, Meister JJ. 1997. Residual strain effects on the stress field in a thick wall finite element model of the human carotid bifurcation. *Journal of Biomechanics*, **30**, 8: 777-786.
- Driessen NJB, Wilson W, Bouten CVC, Baaijens FPT. 2004. A computational model for collagen fibre remodeling in the arterial wall. *Journal of Theoretical Biology*, **226**: 53-64.
- Drugan WJ, Willis JR. 1996. A micromechanics-based nonlocal constitutive equation and estimates of representative volume element size for elastic composites. *J. Mech. Phys. Solids*, **44**, 4: 497-524

- Gasser TC, Holzapfel GA. 2002. A rate-independent elastoplastic constitutive model for biological fiber-reinforced composites at finite strains: continuum basis, algorithmic formulation and finite element implementation. *Computational Mechanics*, **29**: 340-360.
- Gusev, A. 1997. Representative volume element size for elastic composites: a numerical study. *J. Mech. Phys. Solids*, **45**, 9: 1449-1459.
- Hill MR, Duan X, Gibson G, Watkins S, Robertson AM. 2012. A theoretical and non-destructive experimental approach for direct inclusion of measured collagen orientation and recruitment into mechanical models of the artery wall. *Journal of Biomechanics*, **45**: 762-771.
- Hill R. 1963. Elastic properties of reinforced solids: some theoretical principles. *J. Mech. Phys. Solids*, **11**: 357-372.
- Holzapfel GA. 2000. Biomechanics of soft tissue. *Computational Biomechanics*, Paper No. 7, START-Project Y74-TEC
- Holzapfel GA, Gasser TC, Ogden RW. 2001. A new constitutive framework for arterial wall mechanics and a comparative study of material models. *Journal of Elasticity* **61**: 1-48.
- Holzapfel GA, Gasser TC, Stadler M. 2002. A structural model for the viscoelastic behavior of arterial walls: Continuum formulation and finite element analysis. *European Journal of Mechanics A/Solids* **21**: 441-463.
- Holzapfel GA, Ogden RW. 2007. On planar biaxial tests for anisotropic nonlinearly elastic solids. A continuum mechanical framework. *Mathematics and Mechanics of Solids*, **14**: 474-489.
- Horgan CO, Saccomandi G. 2003. A description of arterial wall mechanics using limiting chain extensibility constitutive models. *Biomechanical Modeling of Mechanobiology*, **1**:251-266
- Humphrey JD, Yin FCP. 1987. A new constitutive formulation for characterizing the mechanical behavior of soft tissues. *Biophysics Journal*, **52**: 563-570.
- Itskov M, Aksel N. 2004. A class of orthotropic and transversely isotropic hyperelastic constitutive models based on a polyconvex strain energy function. *International Journal of Solids and Structures*, **41**: 3833-3848.

- Kanit T, Forest S, Galliet I, Mounoury V, Jeulin D. 2003. Determination of the size of the representative volume element for random composites: statistical and numerical approach. *International Journal of Solids and Structure*, **40**: 3647-3679.
- Kroon M, Holzapfel GA. 2008. A new constitutive model for multi-layered collagenous tissues. *Journal of Biomechanics*, **41**: 2766-2771.
- Limbert G. 2011. A mesostructurally-based anisotropic continuum model for biological soft-tissues—Decoupled invariant formulation. *Journal of the Mechanical Behavior of Biomedical Materials*, **4**: 1637-1657.
- Nelson A, Cameron J, Kaihui A, Carbone A, Willoughby S, van den Heuvel C, Martin J, Kennedy D, Worthley S, Worthly M. Proximal aortic stiffness in the paediatric adolescent population. *Journal of Cardiovascular Magnetic Resonance* **13**(Suppl 1): 389.
- Ostoja-Starzewski M. 2002. Microstructural randomness versus representative volume element in thermomechanics. *Journal of Applied Mechanics*, **69**: 25-35.
- Ostoja-Starzewski M. 2006. Material spatial randomness: From statistical to representative volume element. *Probabilistic Engineering Mechanics*, **21**: 112-132.
- Pena E, Alastrue V, Laborda A, Martinez MA, Doblare M. 2010. A constitutive formulation of vascular tissue mechanics including viscoelasticity and softening behavior. *Journal of Biomechanics*, **43**: 984-989.
- Schröder J, Neff P. 2003. Invariant formulation of hyperelastic transverse isotropy based on polyconvex free energy functions. *International Journal of Solids and Structures*, **40**: 401-445.
- Srivastava VK, Gabbert U, Berger H. 2011. Representative volume element analysis for the evaluation of effective material properties of fiber and particle loaded composites with different shaped inclusions. *Mechanics of Time-Dependent Materials and Processes in Conventional and Multifunctional Materials*, **3**: 185-192.
- Stalhand J, Klarbring A, Holzapfel GA. 2011. A mechanochemical 3D continuum model for smooth muscle contraction under finite strains. *Journal of Theoretical Biology*, **268**: 120-130.
- Sun CT, Vaidya RS. 1996. Prediction of composite properties from a representative volume element. *Composites Science and Technology*, **56**:171-179.

Zulliger MA, Fridez P, Hayashi K, Stergiopoulos N. 2004. A strain function for arteries accounting for wall composition and structure. *Journal of Biomechanics*, **37**: 989-1000.